Inkjet Printable Polyaniline Nanoformulations

ARTICLE *in* LANGMUIR · AUGUST 2007

Impact Factor: 4.46 · DOI: 10.1021/la700540g · Source: PubMed

6 AUTHORS, INCLUDING:

Aoife Morrin
Dublin City University
49 PUBLICATIONS **1,586** CITATIONS
SEE PROFILE

Simon Moulton
Swinburne University of Technology
104 PUBLICATIONS **2,169** CITATIONS
SEE PROFILE

Malcolm R Smyth
Dublin City University
202 PUBLICATIONS **6,046** CITATIONS
SEE PROFILE

Gordon Wallace
University of Wollongong
508 PUBLICATIONS **16,712** CITATIONS
SEE PROFILE

Inkjet Printable Polyaniline Nanoformulations

Orawan Ngamna,[†] Aoife Morrin,[‡] Anthony J. Killard,[‡] Simon E. Moulton,[†] Malcolm R. Smyth,[‡] and Gordon G. Wallace*[,†]

ARC Centre of Excellence for Electromaterials Science, Intelligent Polymer Research Institute, University of Wollongong, Northfields Avenue, Wollongong, NSW 2522, Australia, and School of Chemical Sciences, National Centre for Sensor Research, Dublin City University, Dublin 9, Ireland

Received February 23, 2007. In Final Form: May 8, 2007

Aqueous polyaniline (PANI) nanodispersions doped with dodecylbenzenesulfonic acid (DBSA) were synthesized and successfully inkjet-printed using a piezoelectric desktop printer. This paper examines the optimization and characterization of the nanoparticulate formulation for optimal film electrochemistry and stability. PANI nanoparticle synthesis was optimized in terms of the ratio of monomer (aniline) to oxidant (ammonium persulphate, APS) and dopant (DBSA). Particle size, UV−vis spectroscopy, electrochemical, and conductivity analyses were performed on all materials. Optimal synthesis conditions were found to be at a molar ratio of 1.0:0.5:1.2 aniline/APS/DBSA. This resulting nanodispersion showed a uniform particle size distribution of ∼82 nm, and UV−vis analysis indicated a high doping level. These synthetic conditions resulted in the highest conductivity, and the electrochemistry of the resulting films was well-defined and stable. Surface tension analysis and rheological studies demonstrated that the aqueous nanodispersions were suitable for inkjet printing. Successful inkjet printing of these polyaniline nanoparticulate formulations is demonstrated.

1. Introduction

Polyaniline (PANI) has been one of the most extensively studied inherently conducting polymers (ICPs) over the past decade due to its reversible redox and pH switching properties, ease of synthesis, and wide range of potential applications in sensing, electrochromics, and other electronic devices.[1,2]

Several techniques have been used to prepare ultrathin conducting polymer films of controlled thickness, for example, spin-coating, casting, self-assembly, and Langmuir−Blodgett (LB) methods.[3] More recently, other methods being used to pattern conducting polymers are screen[4] and inkjet printing.[5,6] These printing methods are among the most promising in the emerging area of printed organic electronics. Printable organic conducting polymer formulations will have vast implications in this area which incorporates applications such as printed devices (e.g., batteries, light emitting displays, microelectromechanical systems (MEMS), radio frequency identification (RFID) tags, and smart sensors).

However, to date, the printing of conducting polymers has been a challenge. Papers have used functionalized polymeric materials such as poly(3,4-ethylenedioxythiophene) (PEDOT) for printing to render the conducting polymer soluble. On the other hand, commercial inkjet cartridges conventionally use dispersions of pigmented particles.[7] The patterning of materials by printing methods is known to be low-cost, rapid, and precise, while also being highly amenable to scale-up for mass production. Inkjet printing, in particular, is a noncontact printing method, eliminating the possibility of physical contact/damage to the substrate. It requires picoliter volumes for printing, resulting in ultrathin films. It is a precise and accurate printing method normally controlled by conventional computer software.[8] Using a multichannel approach, more than one material can be printed simultaneously via different nozzles,[6] making it a promising technique for complete device manufacture.

The most commonly used technologies in inkjet printing are thermal and piezoelectric. Piezoelectric drop-on-demand methods employ piezoceramic materials that are contained in the printhead. Deformation of the piezoceramic material causes an ink volume change to generate a pressure that overcomes the viscous pressure loss inside the nozzle and the surface tension force from the ink meniscus, so that an ink drop can begin to form at the nozzle.[9] To achieve inkjet printable materials, the viscosity of the dispersions to be printed should be in the range 0.5−40 mPa s to ensure compatibility with the limited power generated by the piezoelectric membrane.[10,11] The surface tension of the ink should be between 20 and 70 dyn cm^{-1}, as it must be high enough to be held in the nozzle without dripping and low enough to allow spreading over the substrate surface to form continuous films.[11] Velocity distributions and shear rates at nozzle orifices are important factors in determining the jetting properties of the ink. The shear rate has been defined as the flow rate of fluid over the cross-sectional area of the nozzle,[12] and the typical shear rate inside the nozzles of drop-on-demand inkjet printers is high (in the range of $500-10^5$ s^{-1}).[13,14] The ink, therefore, must be of

* To whom correspondence should be addressed. Telephone: +61(0)2 4221 3127. Fax: +61(0)2 4221 3114. E-mail: gwallace@uow.edu.au.

[†] University of Wollongong.

[‡] Dublin City University.

(1) Wallace, G. G.; Spinks, G. M.; Kane-Maguire, L. A. P.; Teasdale, P. R. *Conductive Electroactive Polymers: Intelligent Materials Systems*, 2nd ed.; CRC Press: Boca Raton, FL, 2002.

(2) Gerard, M.; Chaubey, A.; Malhotra, B. D. *Biosens. Bioelectron.* **2002**, *17*, 345−359.

(3) Rubinger, C. P. L.; Moreira, R. L.; Cury, L. A.; Fontes, G. N.; Neves, B. R. A.; Meneguzzi, A.; Ferreira, C. A. *Appl. Surf. Sci.* **2006**, *253*, 543−548.

(4) Bao, Z.; Feng, Y.; Dodabalapur, A.; Raju, V. R.; Lovinger, A. J. *Chem. Mater.* **1997**, *9*, 1299−1301.

(5) Sirringhaus, H.; Kawase, T.; Friend, R. H.; Shimoda, T.; Inbasekaran, M.; Wu, W.; Woo, E. P. *Science* **2000**, *290*, 2123−2126.

(6) Setti, L.; Fraleoni-Morgera, A.; Ballarin, B.; Filippini, A.; Frascaro, D.; Piana, C. *Biosens. Bioelectron.* **2005**, *20*, 2019−2026.

(7) Magdassi, S.; Ben Moshe, M. *Langmuir* **2003**, *19*, 939−942.

(8) Kawase, T.; Shimoda, T.; Newsome, C.; Sirringhaus, H.; Friend, R. H. *Thin Solid Films* **2003**, *438*−*439*, 279−287.

(9) Le, H. P. *J. Imaging Sci. Technol.* **1998**, *42*, 49−62.

(10) Gans, B.-J.d.; Schubert, U. S. *Macromol. Rapid Commun.* **2003**, *24*, 659−666.

(11) MicroFab Technologies, Inc. Web site. http://www.microfab.com/equipment/technotes/technote99-02.pdf (accessed Feb 15, 2007).

(12) Zhu, H.; Brazee, R. D.; Reichard, D. L.; Fox, R. D.; Krause, C. R.; Chapple, A. C. *Atomization Sprays* **1995**, *5*, 343−356.

10.1021/la700540g CCC: $37.00
Published on Web 07/06/2007

a suitably low viscosity to withstand the high shear rates inside the nozzle. Particle size is also important. The nozzle size inside Epson printer heads, for example, is ~20−30 μm in diameter,[15] which means that printable materials must be either completely soluble or a stable nanodispersion, otherwise they will aggregate and block the nozzles. Conventional pigment particle sizes in printing inks are in the range of 100−400 nm.[7]

Previously, polyaniline nanofibers were synthesized by a method termed as the "rapid mixing method" by Huang and Kaner.[16] Although the diameter of these fibers was estimated to be just 35 nm, their long fibrillar nature[16] may make them unsuitable for patterning using inkjet printing, as they may become entangled and easily clog the nozzle. This rapid mixing concept was based on using an oxidant (APS) as a limiting reagent with respect to the monomer. Therefore, during polymerization, the oxidant molecules were rapidly consumed by polymerizing the aniline monomer and inducing the formation of nanofibers in their vicinity. Complete depletion of the oxidant resulted in the secondary growth of the fibers being suppressed,[16] resulting in individual fibrillar structures of the polymer. This concept is applied to the synthesis of the PANI nanoparticles in this work, where an emulsion polymerization approach was used (using DBSA as dopant) to induce a spherical nanoparticulate formation. The inherent morphology of PANI-DBSA nanoparticulates was spherical, rather than fibrillar, as the polymer was formed inside the DBSA micelles as shown in our previous work.[17]

The ultimate goal of this work was to optimize the synthesis conditions to achieve high quality, inkjet printable PANI-DBSA nanodispersions. The effect of varying the concentration of the reagents used (monomer, oxidant, and stabilizer) was also examined. Particle size analysis (using the dynamic light scattering (DLS) method), UV−vis spectroscopy, cyclic voltammetry (CV), transmission electron microscopy (TEM), and conductivity were used to characterize the resultant polymer nanodispersions. In addition, surface tension measurements and rheological studies of the PANI nanodispersions were carried out and compared to a commercial Epson ink (used as reference). Using these optimized dispersions, the ability to produce high quality prints using simple desktop inkjet printers has been demonstrated.

2. Materials and Methods

2.1. Materials. Aniline (242284) was purchased from Aldrich and distilled before use. Ammonium peroxydisulfate (APS-215589) and sodium dodecyl sulfate (SDS-L4509) were purchased from Aldrich and used as received. Dodecylbenzenesulfonic acid (DBSA-D0989) was purchased from Tokyo Kasei Kogyo Co., Ltd. Epson black ink was obtained from Epson ink cartridges (T036). Dialysis membranes (D9402; 12 000 molecular weight cutoff) were purchased from Sigma and soaked in Milli-Q water before use. All solutions were prepared using Milli-Q water.

2.2. Instrumentation. Syntheses were performed in a Julabo controlled temperature bath. An Eppendorf centrifuge (5702) was used to separate the large polymer particles from the solution. A three-electrode cell comprising a working electrode, a Ag/AgCl reference electrode, and a Pt wire auxiliary electrode connected to an E-Corder 401 unit with an EDAQ potentiostat was used for all electrochemical experiments. The particle size was determined using a dynamic light scattering (DLS) instrument (Nano-ZS Zetasizer, Malvern Instruments) with 8° angled back scattered light configuration. The morphology of the PANI nanoparticles was observed using TEM (H7000, Hitachi) at 100 keV. UV−visible spectra were measured using a Shimadzu UV-1601 spectrophotometer. Conductivity measurements were performed on cast polymer films using the four-point probe method. An air bearing rheometer (Anton Paar Physica MCR 301) with a MRF-7099 spindle was used for the rheology study. Surface tension was measured using a contact angle system (OCA20, DataPhysics Instruments GmbH).

Table 1. Synthesis Conditions for PANI Nanodispersions

ratio	aniline [M]	APS [M]	DBSA [M]
1.00:0.25:1.60 aniline/APS/DBSA	0.16	0.04	0.25
1.00:0.25:1.20 aniline/APS/DBSA	0.16	0.04	0.19
1.00:0.25:0.80 aniline/APS/DBSA	0.16	0.04	0.13
1.0:0.5:1.6 aniline/APS/DBSA	0.16	0.08	0.25
1.0:1.0:1.6 aniline/APS/DBSA	0.16	0.16	0.25
1.0:0.5:1.2 aniline/APS/DBSA	0.16	0.08	0.19

2.3. Synthesis Method. DBSA, at the required concentration, was dissolved in Milli-Q water (40 mL). APS was dissolved in 20 mL of the DBSA solution. Aniline was added to the remaining DBSA solution (20 mL) and was placed in a water bath at 20 °C. This solution was stirred for 2 min before addition of the APS-DBSA solution, and the mixture was stirred for 2.5 h. After polymerization, 20 mL of 0.05 M SDS was added to the reaction mixture to assist in the centrifugation, as the dispersion was very viscous. The solution was centrifuged at 4400 rpm for 30 min. The supernatant containing the PANI nanoparticles was decanted and then dialyzed against 0.05 M SDS for 42 h with the SDS solution being changed twice. The solution was centrifuged again at 4400 rpm for 30 min to remove the remaining aggregates, and the resulting supernatant material was used for characterization. The synthesis conditions investigated are summarized in Table 1.

2.4. Casting Method. Glassy carbon electrodes (3 mm in diameter) were polished with 1.0, 0.3, and 0.05 μm alumina slurry in sequence and then ultrasonicated in water for 5 min. The polyaniline dispersion (5 μL) was dropped onto the surface of the glassy carbon and allowed to dry in air.

2.5. Inkjet Printing of Nanoparticles. Epson print cartridges (T036 and T037) compatible with the Epson Stylus C45 were cut open and emptied of ink, and the sponge inside was removed. All color tanks of the cartridges (black, cyan, magenta, and yellow) were cleaned thoroughly with deionized water. The chip on the cartridge was then reset using a chip resetter (www.9to6.ie), so that the printer would read the cartridge as full. The polyaniline nanoparticle dispersions were then poured into one or more of the color tanks in the cartridge. All other tanks were left empty. The lid was replaced on top of the cartridge, and the cartridge was inserted back into the printer. The polyaniline ink was used to print the images with computer controlled software (Powerpoint) using the "best photo" print quality at 2880 dots per inch (dpi) from the printer settings.

3. Results and Discussion

Using all of the synthesis conditions described in Table 1, stable dispersions of polyaniline were produced. All polyaniline dispersions were synthesized as the conducting emeraldine salt (ES) form.

3.1. Particle Size Analysis. A TEM image of the polymer synthesized from 1.00:0.25:1.60 aniline/APS/DBSA shows that the emulsion polymerization approach used results in spherical particle formation. The PANI nanoparticles were imaged on a carbon sheet where the particles were measured to be between 30 and 80 nm (Figure 1).

Particle size analysis using DLS was also performed on the PANI nanodispersions where the concentration of APS was varied (Figure 2a). The ratio of aniline/DBSA was kept constant for these measurements at 1.0:1.6. The nanoparticles synthesized from 1.00:0.25 aniline/APS exhibited a unimodal size distribution with a narrow size distribution centered at ~65 nm. Under these

(13) Biehl, S.; Danzebrink, R.; Oliveira, P.; Aegerter, M. A. *J. Sol-Gel Sci. Technol.* **1998**, *13*, 177−182.
(14) Reis, N.; Ainsley, C.; Derby, B. *J. Am. Ceram. Soc.* **2005**, *88*, 802−808.
(15) Calvert, P. *Chem. Mater.* **2001**, *13*, 3299−3305.
(16) Huang, J. X.; Kaner, R. B. *Angew. Chem., Int. Ed.* **2004**, *43*, 5817−5821.
(17) Moulton, S. E.; Innis, P. C.; Kane-Maguire, L. A. P.; Ngamna, O.; Wallace, G. G. *Curr. Appl. Phys.* **2004**, *4*, 402−406.

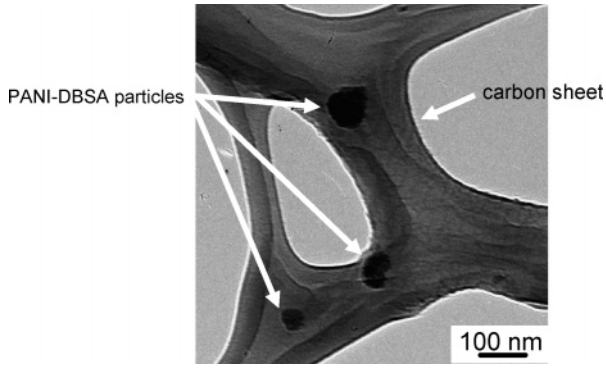

Figure 1. TEM image of PANI nanoparticles synthesized from 1.00:0.25:1.60 aniline/APS/DBSA. The image was obtained at 100 keV at a magnification of ×200K.

conditions, the amount of APS is limiting so that it is consumed rapidly, suppressing secondary growth of the polymer particles. The particle size distribution was found to be bimodal when the ratio of APS was increased to 0.5. On doubling the APS molar concentration (aniline/APS = 1:1), the particle size within the dispersion increased to more than 1000 nm. This was attributed to secondary growth of the polymer particles induced by the presence of excess oxidant.

The effect of DBSA concentration on particle size was also studied. The aniline/DBSA ratios investigated were 1.0:1.6, 1.0:1.2, and 1.0:0.8. The ratio of aniline/APS was kept constant at 1.00:0.25. Increasing the DBSA content stabilized the dispersions and hence minimized the particle size (Figure 2b) where the ratio of 1.0:1.6 aniline/DBSA resulted in the lowest particle size of ∼90 nm. Higher concentrations of DBSA resulted in more stable nanodispersions with smaller particle sizes. However, excessively high levels of the DBSA surfactant may serve to increase the resistivity of the resulting material. The inverse is true for high levels of APS. Increasing the ratio of aniline to APS oxidant from 1:0.5 to 1:1 in the dispersions leads to an increase of ∼10-fold in the particle size. However, maximizing the amount of APS would be expected to be more ideal in terms of optimal conductivity. Nevertheless, the particle size of these dispersions is, in the first instance, more important to enhance their processibility and hence inkjet printability. To find a tradeoff between particle size and conductivity, the effect of increasing the ratio of aniline/APS to 1.0:0.5 while decreasing the DBSA ratio to 1.0:1.2 was investigated. The particle size of this resulting nanodispersion (Figure 2c) showed a small and uniform particle size with a distribution centered at ∼82 nm. Hence, it was possible to synthesize the material with an increased amount of APS while minimizing the amount of DBSA present 1.0:0.5:1.2 aniline/APS/DBSA to maintain a small particle size.

3.2. UV−Vis Spectroscopy. The PANI nanodispersions were diluted in water, and their UV−vis spectra were obtained (Figure 3). The spectra showed the typical characteristics of the conducting emeraldine salt (ES) form of PANI. The $\pi-\pi^*$ band appeared at ∼350 nm, the π-polaron band appeared at 430 nm, and the localized polaron bands appeared in the range of 765−790 nm for samples synthesized under different conditions. These spectra indicated a "coil-like" conformation for the polymer backbone, as the free-carrier tail in the near IR region was absent. This structure causes the polarons of each tetrameric unit in PANI to be electronically isolated from each other due to the twist defects between aromatic rings.[18]

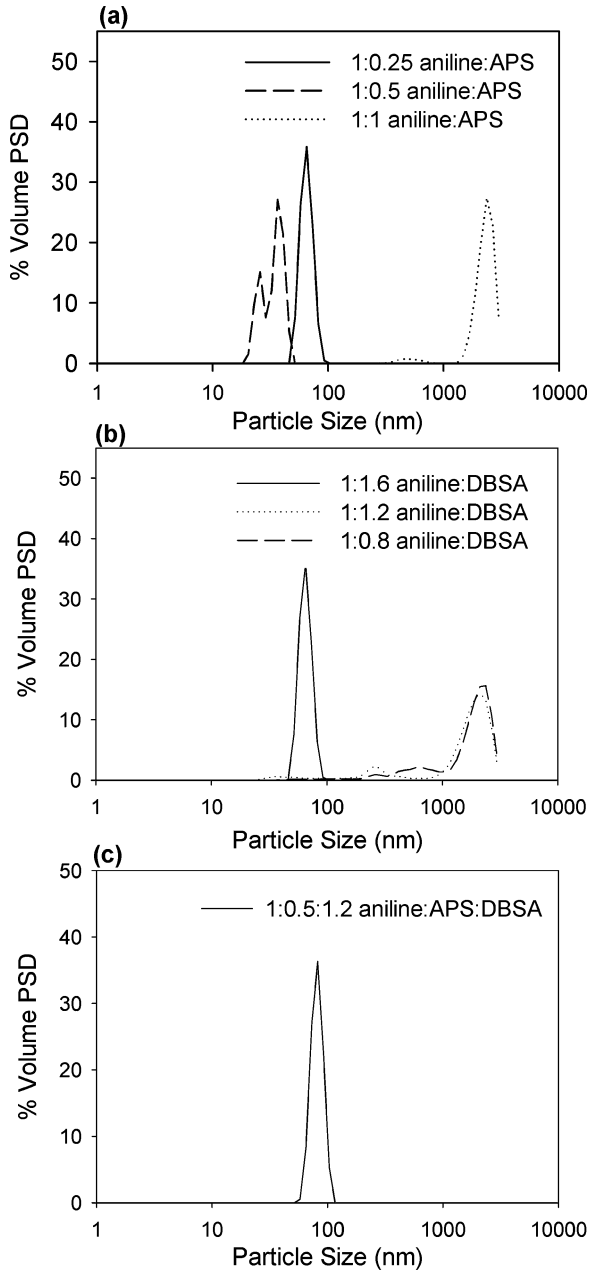

Figure 2. Size distribution of PANI nanodispersions synthesized from (a) various ratios of aniline/APS (the ratio of aniline/DBSA was kept constant at 1.00:1.60), (b) various ratios of aniline/DBSA (the ratio of aniline/APS was kept constant at 1.00:0.25), and (c) 1.00:0.50:1.20 aniline/APS/DBSA.

When the monomer/APS ratio was decreased from 1.00:0.25 to 1:1, the relative intensity of the π-polaron band at 430 nm increased, indicating a higher degree of doping[19] (Figure 3a). Moreover, as the ratio was decreased from 1.00:0.25 to 1.0:0.5 to 1:1, the polaron band shifted from 765 to 770 to 790 nm, respectively, where this shift increase indicates higher conjugation lengths.[20] The increasing intensity of the free-carrier tail in the near IR region indicated the polymer was more likely to be in the "expanded coil" conformation when a lower ratio of aniline/APS was used. In this more expanded conformation, the twist defects between the aromatic rings are removed and the interaction between the adjacent isolated polarons becomes stronger.[18]

(18) Xia, Y.; Wiesinger, J. M.; MacDiarmid, A. G.; Epstein, A. J. *Chem. Mater.* **1995**, *7*, 443−445.

(19) Kim, B. J.; Oh, S. G.; Han, M. G.; Im, S. S. *Synth. Met.* **2001**, *122*, 297−304.

(20) Norris, I. D.; Kane-Maguire, L. A. P.; Wallace, G. G. *Macromol.* **2000**, *33*, 3237−3243.

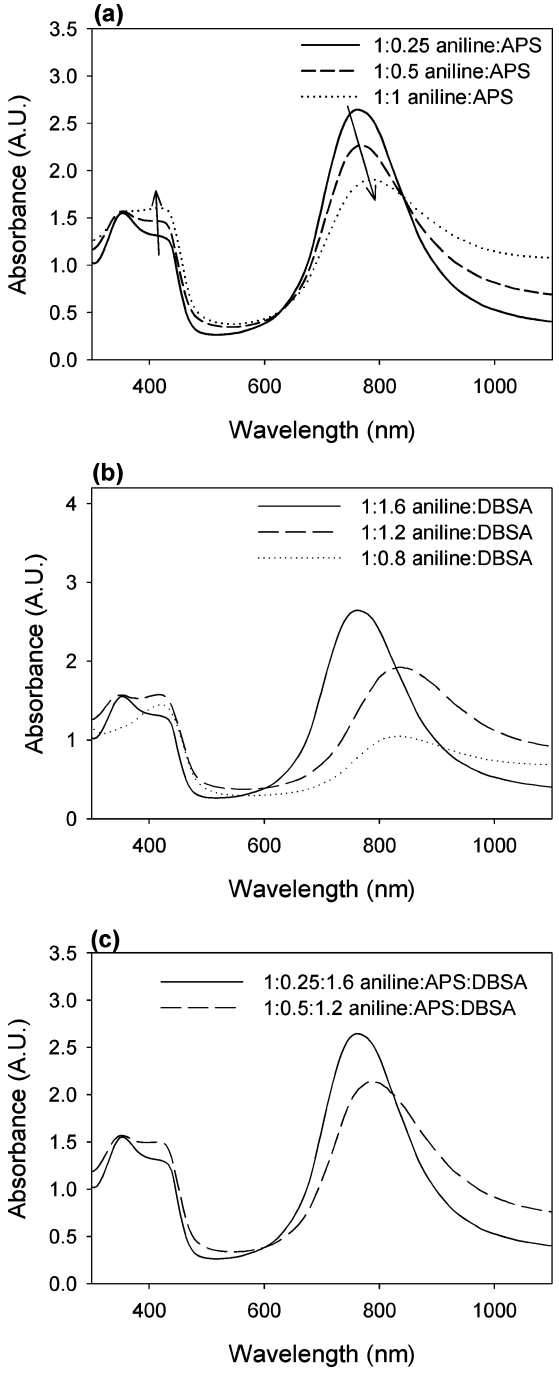

Figure 3. UV−vis spectra of PANI nanodispersions synthesized from (a) various ratios of aniline/APS (the ratio of aniline/DBSA was 1.0:1.6 for all samples), (b) various ratios of aniline/DBSA (the ratio of aniline/APS was 1.00:0.25 for all samples), and (c) 1.00:0.25:1.60 aniline/APS/DBSA and 1.0:0.5:1.2 aniline/APS/DBSA.

When the aniline/DBSA ratio was varied, a significant change in the UV−vis spectra was observed (Figure 3b). The relative intensity of the polaron band at 430 nm to the $\pi-\pi^*$ band at 350 nm increased with increasing ratios of aniline/DBSA, indicating higher doping efficiencies.[21] This result indicated that the ratio of aniline/DBSA to be used in this synthesis should be 1.0:1.2 or lower. Increasing the ratio led to insufficient polymerization as shown in Figure 3c (1.0:0.8 aniline/DBSA).

The UV−vis spectrum of the polymer synthesized from 1.0:0.5:1.2 aniline/APS/DBSA was compared to that of the original recipe of 1.00:0.25:1.60 aniline/APS/DBSA. The relative intensity

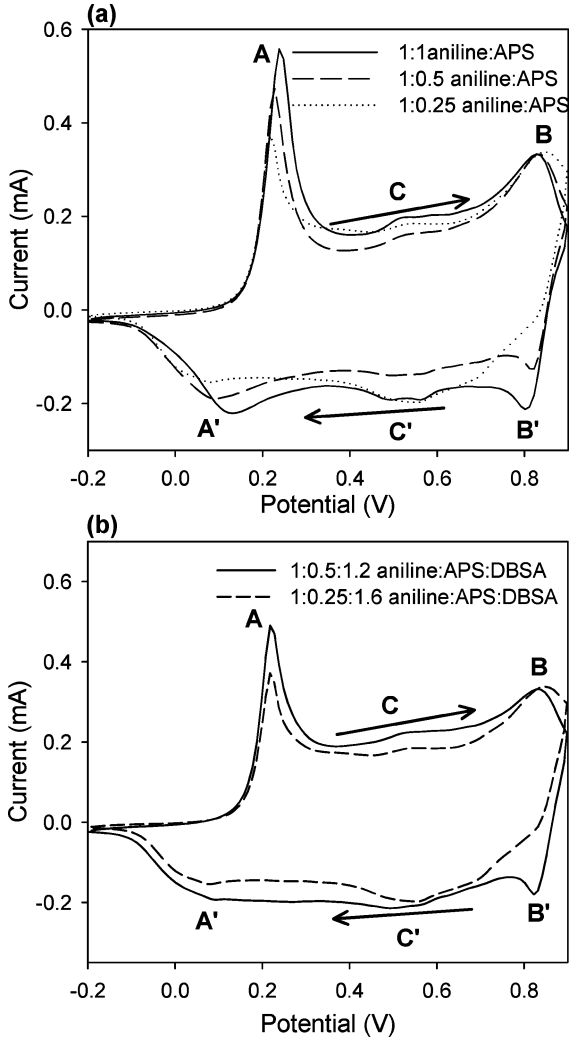

Figure 4. Cyclic voltammograms of PANI nanodispersions cast onto glassy carbon electrodes where the formulations used for casting were synthesized from (a) various ratios of aniline/APS where the ratio of aniline/DBSA was kept at 1:1.6 and (b) 1:0.25:1.6 aniline/APS/DBSA and 1.0:0.5:1.2 aniline/APS/DBSA. Scan rate: 100 mV s^{-1}. Arrows indicate direction of potential scan.

of the π-polaron to the $\pi-\pi^*$ band from PANI nanodispersions synthesized from 1.00:0.25:1.60 aniline/APS/DBSA was higher than that where a ratio of 1.0:0.5:1.2 aniline/APS/DBSA was used, indicating a higher level of doping (Figure 3c). Moreover, the polaron band maxima of the polymer synthesized from 1.0:0.5:1.2 aniline/APS/DBSA appeared at 790 nm, compared to the lower wavelength of 765 nm for the polymer synthesized from 1.00:0.25:1.60 aniline/APS/DBSA, indicating longer conjugation lengths.

3.3. Effect of Synthesis Conditions on the Electrochemistry of Cast PANI-DBSA Films. Cyclic voltammetry (CV) was performed on films obtained by casting the polymer dispersions onto glassy carbon electrodes. The modified electrodes were cycled in HCl (1 M) at a scan rate of 100 mV s^{-1}. The CVs (Figures 4 and 5) show typical PANI redox electrochemistry,[1] with the main peaks A and B corresponding to the transformation of leucoemeraldine (LB) to emeraldine salt (ES) and ES to pernigraniline (PS), respectively. On the reverse scan, peaks B′ and A′ correspond to the conversion of PS to ES and ES to LB, respectively. The presence of peaks C/C′ is associated with the formation of *p*-benzoquinone and hydroquinone[22] as side products

(21) Han, M. G.; Cho, S. K.; Oh, S. G.; Im, S. S. *Synth. Met.* **2002**, *126*, 53−60.

(22) Chen, W. C.; Wen, T. C.; Gopalan, A. *Synth. Met.* **2002**, *128*, 179−189.

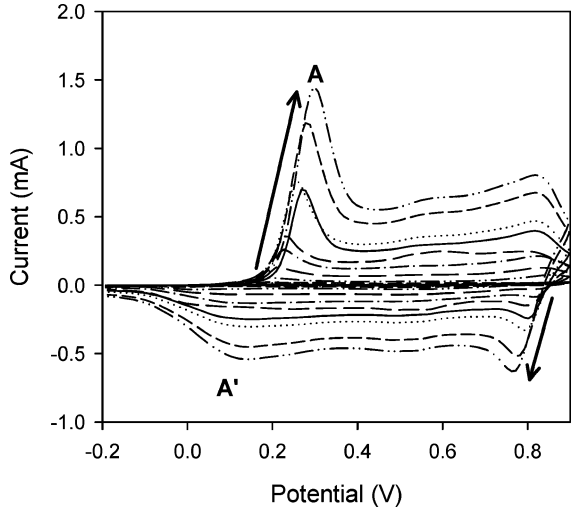

Figure 5. Scan rate study in 1 M HCl of the cast film PANI-DBSA synthesized from 1.0:0.5:1.2 aniline/APS/DBSA.

upon cycling to high oxidative potentials necessary to observe the transition from an ES to a PS couple.[23]

The PANI nanodispersions synthesized using lower ratios of aniline/APS showed more defined electrochemistry, and the relative current magnitude of the C/C′ redox couples was lower than those of the A/A′ and B/B′ couples (Figure 4a), indicating better redox switching processes and more stable polymer films. Similar effects for the polymer synthesized from different DBSA concentrations was found. Increasing the concentration of DBSA resulted in CVs with greater definition (data not shown).

The voltammogram of the polymer synthesized from 1.0:0.5:1.2 aniline/APS/DBSA was better than that of the polymer synthesized using the original formulation of 1.00:0.25:1.60 aniline/APS/DBSA (Figure 4b) in terms of peak definition. Little or no oxidative activity was observed for the ES transition (peak B′) in films synthesized from the original formulation, whereas a well-defined peak was observed for the 1.0:0.5:1.2 aniline/APS/DBSA formulation. Moreover, the relative current magnitude of the degradation products (C/C′ couples) to the PANI characteristic peaks (A/A′ and B/B′ couples) was lower when the polymer was synthesized from 1.0:0.5:1.2 aniline/APS/DBSA, indicating a more stable polymer.

A scan rate study of the cast film of the PANI-DBSA nanodispersion synthesized from a molar ratio of 1.0:0.5:1.2 aniline/APS/DBSA was performed, and the peak currents of the A/A′ couples were plotted against the scan rate. A linear relationship ($r^2 = 0.9989$ and 0.9974, respectively, for peaks A and A′) between the scan rate and the peak current indicated that the redox reaction was due to a surface-confined species.[24]

3.4. Electrical Conductivity. Conductivity measurements of cast polymer films were performed using the four-point probe method (Table 2). The higher the proportion of APS used, the higher the conductivity obtained which could be attributed to a more efficient oxidation process during synthesis. This correlates with the electrochemical data, where the higher the ratios of APS used resulted in increased peak heights for each of the polyaniline peaks (Figure 4), indicating improved redox characteristics of the film. It also correlates to the UV−vis spectra (Figure 3a), where increased amounts of APS resulted in a polaron band shift due to higher conjugation lengths. This would serve to increase the overall conductivity of the dispersion. Where a ratio of 1:1 aniline/APS was used, the conductivity was highest at 32.8 ± 7.4 mS s^{-1}. However, this high level of APS results in a large particle size (Figure 1a) and hence is not inkjet printable. Higher DBSA proportions resulted in lower conductivity due to either the insulating effect of this surfactant and/or a composite effect due to the increased size of the composite. Incorporation of conducting materials such as gold nanoparticles or single-walled carbon nanotubes (SWNTs) into the polyaniline dispersions would help counteract the insulating effect of the DBSA and enhance the overall conductivity.

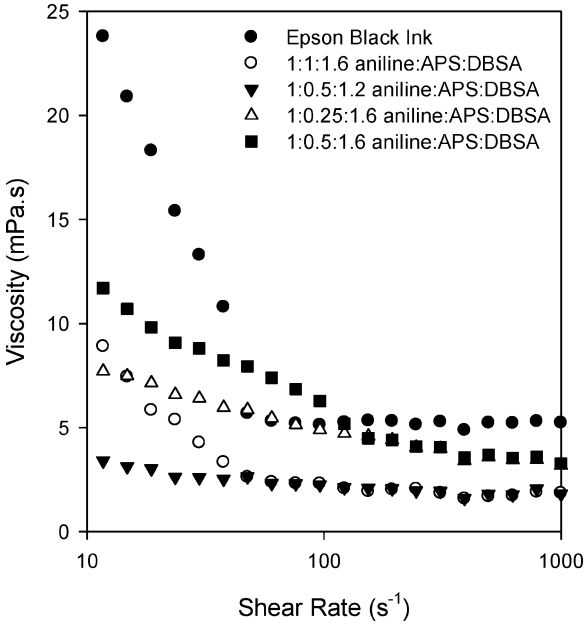

Figure 6. Rheological study of the PANI-DBSA nanodispersions and a commercial Epson ink (T038).

Table 2. Bulk Conductivity Measurements of PANI Nanodispersions (n = 3, Measurements Taken at Different Points on Single Films)

formulation	conductivity (mS cm^{-1})
1.00:0.25:1.60 aniline/APS/DBSA	0.8 ± 0.1
1.0:0.5:1.6 aniline/APS/DBSAA	2.2 ± 0.2
1.0:1.0:1.6 aniline/APS/DBSA	32.8 ± 7.4
1.0:0.5:1.2 aniline/APS/DBSA	4.3 ± 0.6

Table 3. Surface Tension Data for PANI Nanodispersions and Commercial Epson T038 Ink

formulation	surface tension (dyn cm^{-1})
1.00:0.25:1.56 aniline/APS/DBSA	27 ± 0.1
1.00:0.50:1.56 aniline/APS/DBSA	27 ± 0.0
1.00:1.00:1.56 aniline/APS/DBSA	29 ± 0.1
1.00:0.50:1.19 aniline/APS/DBSA	28 ± 0.1
Epson black ink (T038)	30 ± 0.1

3.5. Surface Tension and Rheological Studies. The surface tension of each of the PANI-DBSA nanodispersions was measured and compared to the Epson T038 black ink as shown in Table 3. All dispersions exhibited surface tensions in a range suitable for inkjet printing (20−70 dyn cm^{-1}),[11] although all were slightly below the surface tensions of a commercial Epson ink (T038).

A rheological study of the polymer nanodispersions and the Epson T038 ink was also performed, and the results are shown in Figure 6. At high shear rates (> 500 s^{-1}), the PANI-DBSA dispersions and Epson T038 ink were comparable and behaved as Newtonian fluids. High shear rates are required inside the piezoelectric printhead nozzles (500−10^5 s^{-1}).[13,14] At lower shear rates, Epson T038 appears to be non-Newtonian in nature,

(23) Mirmohseni, A.; Wallace, G. G. *Polymer* **2003**, *44*, 3523−3528.
(24) Do, J. S.; Chang, W.-B. *Sens. Actuators, B* **2004**, *101*, 97−106.

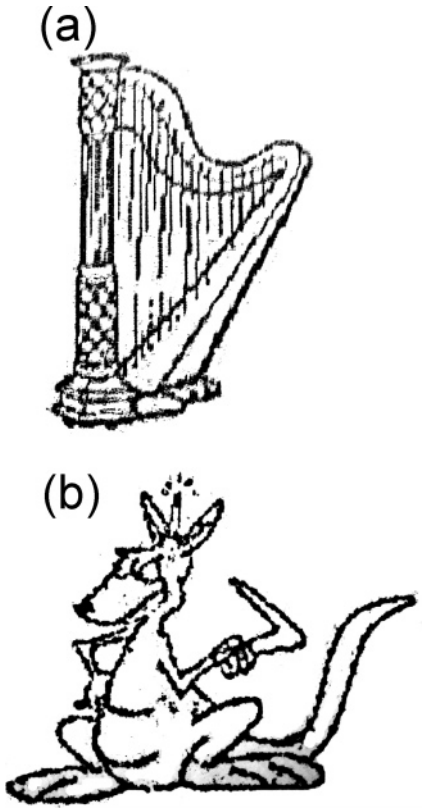

Figure 7. Photographic images of inkjet printed patterns on paper fabricated using the polyaniline nanoparticle dispersion as the deposition ink from a piezoelectric Epson C45 printer: (a) an Irish harp (50×30 mm^2) and (b) an Australian kangaroo (40×35 mm^2).

exhibiting shear thinning which is an ideal ink property. The PANI inks deviate slightly from Newtonian, showing moderately higher viscosity at low shears. Moreover, the viscosities of all of the PANI-DBSA nanodispersions are in the suitable range for inkjet printing (0.5−40 mPa s),[10,11] although they were considerably lower than the viscosity of the Epson T038 ink when shear rates lower than 500 s^{-1} were applied.

3.6. Inkjet Printing. Printing of the polyaniline nanoparticle dispersions was carried out according to the Methods Section using a piezoelectric-based Epson Desktop C45 printer. Figure 7 shows two images that were printed onto standard paper using the polyaniline nanodispersion ink. At 2880 dpi, very high-resolution images could be achieved. The drawings, which were $\sim 40 \times 30$ mm, took about 30 s to print. This demonstrates the feasibility of using these types of material formulations as inks for printing. Inkjet printing is a method that is simple, rapid, and inexpensive. Coupled with conducting nanoparticulate inks such as these polyaniline nanodispersions, it holds much potential for the development of low cost, printed electronic devices.

Bulk conductivity measurements were taken on inkjet printed films (20 prints, 1 cm^2) using a standard four-point probe. The films generated resulted in a conductivity of 0.4 mS cm^{-1} ($n =$ 3, measurements taken at different points on the films) for films fabricated using the 1.00:0.25:1.60 aniline/APS/DBSA formulation. This demonstrates that very thin inkjet printed films possess conductivities of approximately the same order of magnitude as that of much thicker, drop-coated films (0.8 ± 0.1 mS cm^{-1}, Table 2). This, in conjunction with the level of control that can be obtained by inkjet printing and its amenability to mass production and low material consumption, makes it an ideal fabrication methodology for the deposition of inkjet printable formulations of conducting polymer nanoparticles for the production of flexible, printed electronics.

4. Conclusion

The aim of this work was to develop a suitable conducting aqueous-based polyaniline ink for application in piezoelectric inkjet printing. A range of synthetic conditions were investigated where the ratios of both oxidant and dopant to monomer were varied. The optimal synthetic conditions of these PANI-DBSA nanodispersions were found to be at a ratio of 1.0:0.5:1.2 aniline/APS/DBSA. This dispersion showed a uniform particle size distribution of ∼82 nm, observed using DLS. UV−vis analysis indicated a high doping level with a compact coil formation. Electrochemistry of these dispersions was well-defined and stable. The bulk conductivity of these films (1.0:0.5:1.2 aniline/APS/DBSA) was reported to be 4.3 ± 0.6 mS cm^{-1}. A rheological study indicated that all PANI-DBSA nanodispersions synthesized had viscosities suitable for piezoelectric inkjet printing. Surface tensions of the nanodispersions were also similar to that of a commercial inkjet printing ink. Inkjet printing of the nanoparticles was successfully carried out using an Epson Stylus C45 printer. High quality images were generated in just 30 s, demonstrating that inkjet printing as a deposition method for conducting polymer nanomaterials has excellent potential in areas such as printed electronics and sensors.

Acknowledgment. The authors wish to acknowledge the financial support of the Australian Research Council (through the ARC Centre of Excellence program) and Enterprise Ireland under the Technology Development Fund TD/03/107.

LA700540G